Synthesis and Characterization of Tungsten Amide Complexes for the Deposition of Tungsten Disulfide Thin Films

Ji Young Son,[⊥] Su Han Kim,[⊥] Ji Min Seo, Jongsun Lim, Taek-Mo Chung, and Bo Keun Park*

Cite This: *ACS Omega* 2023, 8, 19816−19821

Read Online

ACCESS | Metrics & More | Article Recommendations | SI Supporting Information
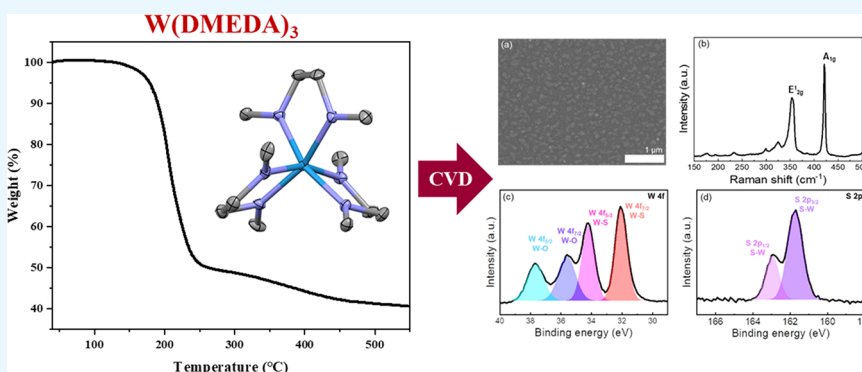
ABSTRACT: To substitute corrosive halogen ligands, we designed and synthesized novel tungsten complexes containing amido ligands, W(DMEDA)$_3$ (**1**) and W(DEEDA)$_3$ (**2**) (DMEDA = *N,N′*-dimethylethylenediamido; DEEDA = *N,N′*-diethylethylenediamido). Complexes **1** and **2** were characterized by ^{1}H NMR, ^{13}C NMR, FT-IR, and elemental analysis. The pseudo-octahedral molecular structure of **1** was confirmed by single-crystal X-ray crystallography. The thermal properties of **1** and **2** were analyzed by thermogravimetric analysis (TGA), which confirmed that the precursors were volatile and exhibited adequate thermal stability. Additionally, the WS$_2$ deposition test was performed using **1** in thermal chemical vapor deposition (thermal CVD). Further analysis of the surface of the thin films was conducted using Raman spectroscopy, scanning electron microscopy (SEM), and X-ray photoelectron spectroscopy (XPS).

INTRODUCTION

Thin films consisting of tungsten (W) and its complexes, including oxides, nitrides, sulfides, and carbides, offer remarkable qualities such as high electrical conductivity, superior thermal stability, high corrosion resistance, and high hardness values.[1] These properties are useful in a variety of fields, including MOL (middle-of-line) local interconnects,[2] photocatalysis,[3] DRAM (dynamic random access memory) word lines and bit lines,[4] supercapacitor applications,[5] and solar cells.[6] Tungsten sulfide (WS$_x$) and two-dimensional (2D) transition metal dichalcogenides (TMDs; MX$_2$/M: Mo, W, Nb; X: S, Se, Te)[7−10] have excellent optical characteristics and an adjustable bandgap between 2.41 and 3.11 eV[11] and have been used for a variety of applications, including transistors, optoelectronics, lithium-ion batteries, biosensors, and chemical sensors.[12]

CVD and atomic layer deposition (ALD) methods have been used to deposit W-based thin films. In particular, WS$_2$ thin films have been deposited using precursors such as W(CO)$_6$, WF$_6$, WCl$_6$, and WO$_3$ by the CVD process. The ALD process yields high uniformity, excellent reproducibility, and accurate film thickness control and can form extremely thin WS$_2$ films with enhanced properties. ALD processes using

WF$_6$ and H$_2$S are well known; however, using tungsten halide as a precursor in this process results in toxic and corrosive byproducts such as HF.[13] To avoid this issue, halogen-free tungsten precursors are required for the deposition of W-based thin films. As an example, low-temperature deposition of WS$_2$ thin films using W(N^{t}Bu$_2$)$_2$(NMe$_2$)$_2$ and H$_2$ + H$_2$S plasma by PEALD (plasma-enhanced atomic layer deposition) has been reported.[14] In a different way, synthesis of single-source precursors such as WS(S$_2$)(S$_2$CNEt$_2$)$_2$,[15] W(SEtN(*Me*)-EtS)$_2$,[16] and (WSCl$_4$)$_2$(^{i}PrS(CH$_2$)$_2$S^{i}Pr)[17] and WS$_2$ thin-film deposition using these precursors have been reported. A comparison for two methods of 2D TMDC formation using single-source precursors containing chalcogens and multi-source precursors requiring additional chalcogen sources

Scheme 1. Synthesis of Complexes 1 and 2
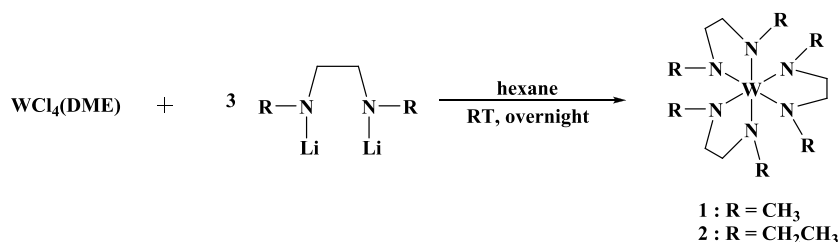
(sulfur, H_2S, etc.) has recently been reported.[18] However, there is still a lot of research to be done on both approaches.

Because O-containing ligand-bound precursors are more likely to form oxide layers, we thought of an all-nitrogen-bound ligand that is highly reactive and oxygen-free. Additionally, it is anticipated that all-nitrogen-bound ligands will make it possible to introduce universal precursors that can build a variety of W-containing thin films. The ligands employed in all-nitrogen-bound W precursors included nitride, imido, amido, guanidinato, and amidinato moieties. W-$(N^tBu)_2[(^iPrN)_2CMe]_2$,[19] $W(N^tBu)_2(NMe_2)$-$[(^iPrN)_2CNMe_2]$,[20] $W(N^tBu)_2(H)[(^iPrN)_2CNMe_2]$,[20] WN-$(NMe_2)[(N^iPr)_2C(NMe_2)]_2$,[21] and $W_2(NMe_2)_6$[22] are previously reported nitrogen-bound W precursors. These precursors are either nonvolatile or volatile only at high temperatures (that is, >130 °C). Designing precursors with volatility at low temperatures is, therefore, critical to compensate for these shortcomings. As an effective strategy, chelating amido ligands capable of achieving thermal stability while maintaining volatility and reactivity better than common amido ligands such as dimethylamido ligands have been proposed.

The same ligand was used in the previously synthesized $W_2(MeNCH_2CH_2NMe)_3$;[23] however, the reported W complex was a dimer, which is difficult to use as a precursor in terms of volatility. The main difference is that the synthesis precursors, $W(DMEDA)_3$ (**1**) and $W(DEEDA)_3$ (**2**) (DMEDA = *N,N′*-dimethylethylenediamido; DEEDA = *N,N′*-diethylethylenediamido), were monomers and were volatilized. Precursor **1** was successfully used to deposit WS_2 thin films from S powder via thermal CVD.

■ RESULTS AND DISCUSSION

Synthesis and Characterization. The reaction of 2 equiv of $MeNLi(CH_2)_2LiNMe$ (Li$_2$(DMEDA)) with tetravalent $WCl_4(DME)$ was supposed to produce tetravalent W-$(DMEDA)_2$, but instead, hexavalent $W(DMEDA)_3$ (**1**) was produced in a low yield of 39%. Referring to this result, the yield increased to 76% when Li$_2$(DMEDA) was reacted using 3 equiv (Scheme 1). Even when hexavalent WCl_6 was reacted with 3 equiv of Li$_2$(DMEDA), complex **1** was still produced in a yield of 53%. The reaction of $WCl_4(DME)$ and 3 equiv of Li$_2$(DMEDA) was the best procedure in terms of yield. Accordingly, $W(DEEDA)_3$ (**2**) was also synthesized in a yield of 52% by reacting $WCl_4(DME)$ with 3 equiv of EtNLi-$(CH_2)_2LiNEt$ (Li$_2$(DEEDA)) (Scheme 1). On the other hand, $W_2(MeNCH_2CH_2NMe)_3$, a dimer structure in which the same ligand is bound, was synthesized in a yield of 64% by reacting with $MeNLi(CH_2)_2LiNMe$ using $W_2Cl_2(NMe_2)_4$ as a starting material.[23] Complexes **1** and **2** were purified as red solids by sublimation at 70 and 75 °C under 450 mTorr, respectively. The two complexes are soluble in organic solvents such as benzene, toluene, hexane, ether, and THF.

Crystal Structure. At a low temperature, crystals suitable for X-ray structure determination were grown in a concentrated diethyl ether solution of **1** at −20 °C. Complex **2** did not crystallize despite several trials. The crystallographic data for **1** are provided in Table 1, and selected bond lengths and bond angles are shown in Table 2.

Table 1. Crystallographic Data and Data Collection Parameters for 1[a]

empirical formula	$C_{12}H_{30}N_6W$
formula weight	442.27
temperature [K]	100(1)
wavelength [Å]	0.71073
crystal system	tetragonal
space group	$I4_1/acd$
a [Å]	16.7170(8)
b [Å]	16.7170(8)
c [Å]	23.5109(16)
α [°]	90
β [°]	90
γ [°]	90
volume [Å^3]	6570.3(8)
Z	16
density (calculated) [Mg/m^3]	1.788
absorption coefficient [mm^{-1}]	7.031
$F(000)$	3488
crystal size [mm^3]	0.140 × 0.100 × 0.100
theta range for data collection [°]	2.437 to 25.991
index ranges	$-20 \leq h \leq 20$, $-20 \leq k \leq 20$, $-28 \leq l \leq 28$
reflections collected	46,129
independent reflections [R(int)]	1562 [0.0305]
completeness to theta = 25.242° [%]	96.3
max. and min. transmission	0.54 and 0.42
data/restraints/parameters	1562/0/91
goodness-of-fit on F^2	1.205
final R indices [$I > 2$sigma(I)]	$R1 = 0.0130$, $wR2 = 0.0297$
R indices (all data)	$R1 = 0.0145$, $wR2 = 0.0303$

[a]$R1 = \Sigma(||F_o| - |F_c||)/\Sigma|F_o|$. $wR2 = \Sigma\{w(F_o^2 - F_c^2)^2/\Sigma[w(F_o^2)^2]\}^{1/2}$.

As shown in Figure 1, the crystal structure of **1** reveals a pseudo-octahedral geometry with amido ligands. The W−N1, W−N2, and W−N3 bond lengths are 2.0096(17), 2.0129(17), and 2.0123(18) Å, respectively, slightly longer than the distances observed for previously reported amide tungsten complexes (1.95−1.97 Å).[24] Through this result, it is confirmed that tungsten in this complex has a hexavalent oxidation state.

The sum of the bond angles around N1 (359.91°), N2 (359.71°), and N3 (359.83°) in **1** is approximately 360°, indicating the sp^2 hybridization of the amide nitrogen atom.[24]

Table 2. Selected Bond Lengths (Å) and Angles (°) for 1

bond length (Å)			
W(1)−N(1)	2.0096(17)	W(1)−N(2)	2.0129(17)
W(1)−N(3)	2.0123(18)		
bond angle (°)			
N(1)−W(1)−N(2)	77.12(7)	N(3)−W(1)−N(3)′	76.79(10)
N(1)−W(1)−N(3)	162.23(8)	N(2)−W(1)−N(2)′	160.54(10)
C(1)−N(1)−W(1)	118.90(13)	C(3)−N(1)−W(1)	128.87(14)
C(1)−N(1)−C(3)	112.14(18)	C(2)−N(2)−W(1)	118.01(14)
C(4)−N(2)−W(1)	129.29(14)	C(2)−N(2)−C(4)	112.41(18)
C(5)−N(3)−W(1)	119.92(14)	C(6)−N(3)−W(1)	128.45(15)
C(5)−N(3)−C(6)	111.46(18)	N(1)−C(1)−C(2)	106.56(18)
N(2)−C(2)−C(1)	107.28(19)	N(3)−C(5)−C(5)′	107.37(12)
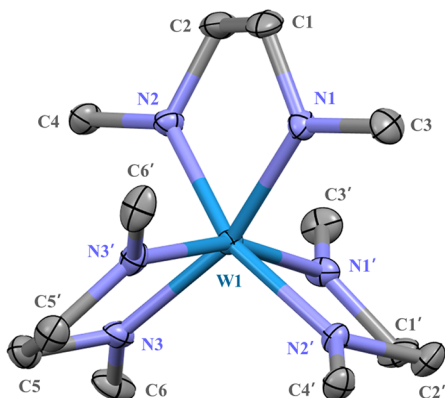
Figure 1. Thermal ellipsoid diagram of the crystal structure of **1**. Thermal ellipsoids for non-H atoms are shown at the 25% probability level.

The bond angles of N1−W−N3 and N2−W−N2′ are 162.23(8)° and 160.54(10)°, respectively, deviating from the ideal angle of 180° with respect to the axial position of the octahedron.

The bidentate di-amido ligands together with the tungsten atom form the five-membered metallacycles, W1−N1−C1−C2−N2 and W1−N3−C5−C5′−N3′, with N1−W−S1 and N3−W1−N3′ bond angles of 77.12(12)° and 76.79(10)°, respectively. The bond angles of W1−N1−C1, N1−C1−C2, C1−C2−N2, and C2−N2−W1 are 118.90(14)°, 106.56(2)°, 107.28(2)°, and 118.01(15)°, respectively, for the W1−N1−C1−C2−N2 metallacycle. In the case of the W1−N3−C5−C5′−N3′ metallacycle, the bond angles are 119.92(14)° (W1−N3−C5), 107.37(12)° (N3−C5−C5′), 107.37(12)° (C5−C5′−N3′), and 119.92(14)° (C5′−N3′−W1). The sum values of the angles were 527.87(9)° and 531.37(12)° compared with the sum of the ideal angles (540°) of a pentagon, owing to the metallacycle envelope conformation.[25]

Thermogravimetric Analysis. TGA of **1** and **2** was conducted from room temperature to 550 °C under a constant flow of argon gas. TGA of **1** shows a single-step evaporation between 180 and 236 °C. At 263 °C, approximately 50% weight loss was observed (Figure 2), and the total weight loss of **1** was approximately 59%, which corresponds to the loss of all ligands decomposed (calcd loss of ligands: about 58%). However, the weight loss of **2** began around 100 °C and exhibited multistep decomposition behavior up to 350 °C, with a residual mass of 28% (Figure 2).

Among the all-nitrogen-bonded W precursors, weight losses in W(N^{t}Bu)$_2$[(^{i}PrN)$_2$CMe]$_2$, W(N^{t}Bu)$_2$(NMe$_2$)-
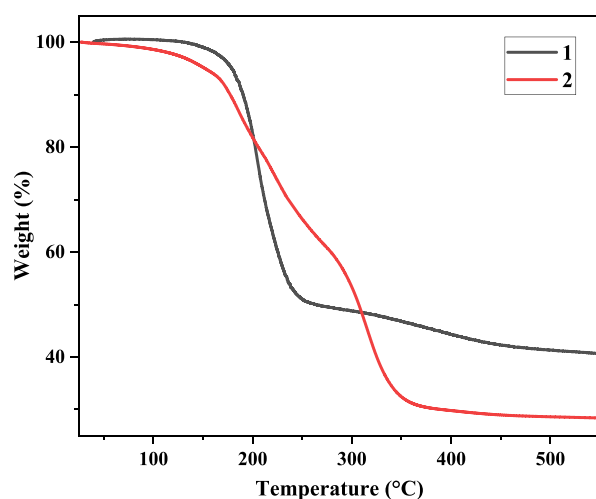
Figure 2. TGA plot of complexes **1** and **2**.

[(^{i}PrN)$_2$CNMe$_2$], W(N^{t}Bu)$_2$(H)[(^{i}PrN)$_2$CNMe$_2$], and WN-(NMe$_2$)[(N^{i}Pr)$_2$C(NMe$_2$)]$_2$ appeared at 100−350, 105−370, 175−370, and 125−200 °C, respectively.[19−21] The amounts of residual mass were approximately 63, 10, 25, and 22%, respectively.[19−21] Unlike non-sublimate WN(NMe$_2$)-[(N^{i}Pr)$_2$C(NMe$_2$)]$_2$, W(N^{t}Bu)$_2$[(^{i}PrN)$_2$CMe]$_2$, [(^{i}PrN)$_2$CNMe$_2$], and W(N^{t}Bu)$_2$(H)[(^{i}PrN)$_2$CNMe$_2$] were sublimed at 130 °C (1 mTorr), 100 °C (10^{-3} mbar), and 100 °C (10^{-3} mbar), respectively.[19−21] Furthermore, W$_2$(MeNCH$_2$CH$_2$NMe)$_3$[23] is a W complex in which the same ligand is bound but is a nonvolatile dimer. However, in the case of **1** and **2**, although the residual masses were rather high at 40 and 28%, respectively, the sublimation temperatures were significantly lower at 70 and 75 °C under 450 mTorr, respectively.

In DSC of **1** and **2**, the endotherms at 119 and 161 °C are similar to the melting points (107−120 and 153−157 °C) of the complexes, respectively (Figure S5). Complex **1** exhibited exothermic events at 196 and 230 °C, suggesting that two decompositions occurred (Figure S5). In the case of **2**, it appears to be an exotherm caused by decomposition at 261 °C (Figure S5).

1 and **2** have comparable or better volatility and thermal stability than the above-mentioned all-nitrogen-bonded W precursors. Accordingly, **1**, which sublimes at lower temperatures and single-step weight loss, was proposed as a suitable precursor for W-based thin-film deposition, and WS$_2$ thin-film deposition was performed.

Deposition and Properties of WS$_2$ Using Complex 1. Large-area WS$_2$ thin films were grown on a Si/SiO$_2$ substrate for 1 h at 700 °C by the CVD method using precursor **1** and sulfur powder (Figure S6). The SEM image in Figure 3a shows that WS$_2$ was uniformly deposited on the substrate. Figure 3b shows the Raman spectra of the WS$_2$ film using 523 nm laser excitation. Two strong peaks appeared at 353 and 421 cm^{-1} derived from the in-plane vibrational E$^1_{2g}$ mode and the out-of-plane vibrational A$_{1g}$ mode of WS$_2$, and the gap of two peaks (67.1 cm^{-1}) indicated that more than 10 layers of films were grown.

The XPS spectra in Figure 3c,d show the chemical composition of WS$_2$ films. The XPS core level spectra of W showed two W 4f doublets corresponding to W−S bonding (32.1 and 34.2 eV) and W−O bonding (35.6 and 37.7 eV)
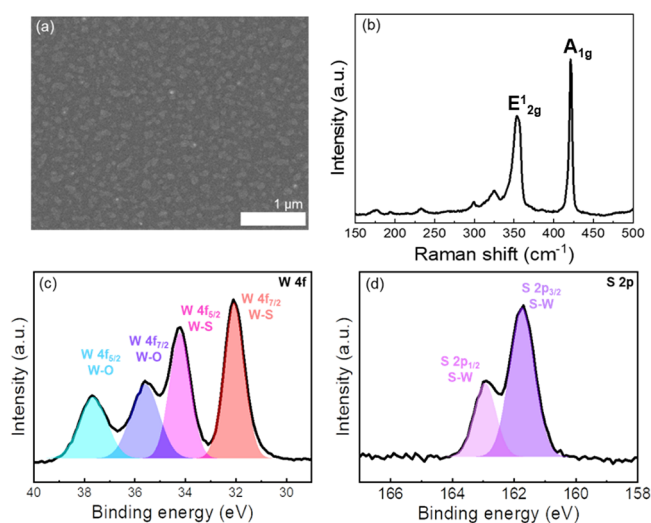
Figure 3. (a) SEM, (b) Raman, and (c, d) XPS spectra of WS_2.

states. These results indicated that some parts of the film were oxidized during the growth process. This is probably caused by some of the precursors being oxidized while putting the precursors into the CVD tube. Two major peaks of the S 2p doublet were obtained at 162.2 and 163.42 eV from W−S bonding.

CONCLUSIONS

In summary, as precursors for W-based materials or thin films, we synthesized novel volatile W-amido complexes, W-$(DMEDA)_3$ (**1**) and $W(DEEDA)_3$ (**2**). The crystal structure of **1** is pseudo-octahedral because it contains the same diamine ligand as the homoleptic complex. Through TGA, the thermal characteristics of **1** and **2** were confirmed. Complexes **1** and **2** were found to have improved volatility and thermal stability compared to previously reported all-nitrogen-bound W precursors. The successful growth of the WS_2 thin film through CVD using **1** was confirmed by the Raman spectra and SEM images. In addition, the complexes are expected to be universally used for various W-containing thin films such as WO_x, WN_x, etc.

EXPERIMENTAL SECTION

General Comments. All materials were handled in an inert atmosphere (Ar) glovebox or using standard Schlenk techniques (N_2). All reaction solvents were dried and deoxygenated using an Innovative Technology PS-MD-4 solvent purification system and stored over activated 3 Å molecular sieves. DMEDA (98%), DEEDA (95%), and tungsten(VI) chloride (99.9%) were purchased from Sigma-Aldrich and purified. WCl_4(DME) (DME = dimethoxyethane) was synthesized using a previously reported procedure in the literature.[26] The ^1H and ^{13}C NMR spectra were recorded using a Bruker Advance NEO 500 MHz FT-NMR spectrometer. All samples for the NMR spectra were sealed in an NMR tube containing C_6D_6 as internal standards inside the Ar atmosphere glovebox. The Fourier-transform infrared (FT-IR) spectra were obtained using a Shimadzu IRSpirit FT-IR spectrophotometer. Samples were prepared within the glovebox using pellets with KBr. Elemental analysis was performed using a Thermo Scientific FLASH EA-2000 organic elemental analyzer.

Synthesis of Tris-η^2-N,N′-dimethylethylenediamino-tungsten ($W(\eta^2$-MeN(CH₂)₂NMe)₃, W(DMEDA)₃) (1). Method A: 1.6 M n-butyllithium (4.125 mL, 6.6 mmol) was added to a 100 mL Schlenk flask containing 10 mL of n-hexanes and DMEDA (264 mg, 3.0 mmol) at −78 °C under a nitrogen atmosphere. The solution was stirred at −78 °C for 30 min and then warmed to room temperature, at which it was further stirred for 5 h. The prepared MeNLi(CH₂)₂LiNMe mixture was then added dropwise to WCl_4(DME) (415 mg, 1 mmol) in hexane (10 mL) at room temperature and stirred overnight. After filtration, a dark red filtrate was recovered. The filtrate was evaporated under the vacuum to afford a red solid $W(\eta^2$-MeN(CH₂)₂NMe)₃ (336 mg, 76% yield) [using DMEDA (2 equiv): yield (174 mg, 39.3%)]. The complex was further purified by sublimation at 70 °C under 450 mTorr. Data for $W(\eta^2$-MeN(CH₂)₂NMe)₃: ^1H NMR (C_6D_6, 500 MHz): δ 4.18 (br, m, 6H, CH₃N(CH_2)₂−), 3.50 (m and s, 24H, CH₃N(CH_2)₂− and CH_3N−). ^{13}C NMR (C_6D_6, 125.7 MHz): δ 64.4 (CH_3N−), 47.1 (CH₃N(CH_2)₂−). Anal. calcd for $C_{12}H_{30}N_6W$: C, 32.59; H, 6.84; N, 19.00. Found: C, 31.61; H, 6.74; N, 17.85. Melting point: 107−120 °C.

Method B: To a 100 mL Schlenk flask containing DMEDA (264 mg, 3.0 mmol) in 10 mL of n-hexanes, 1.6 M n-butyllithium (4.125 mL, 6.6 mmol) was added at −78 °C under a nitrogen atmosphere. The solution was stirred at −78 °C for 30 min, then warmed to room temperature, and further stirred at room temperature for 5 h. The MeNLi(CH₂)₂LiNMe mixture was then added dropwise to WCl_6 (397 mg, 1 mmol) in 10 mL of hexane at room temperature and stirred overnight. After filtration, a dark red filtrate was recovered. The filtrate was evaporated under the vacuum to afford a red solid $W(\eta^2$-MeN(CH₂)₂NMe)₃ (235 mg, 53.2% yield).

Synthesis of Tris-η^2-N,N′-diethylethylenediamino-tungsten ($W(\eta^2$-EtN(CH₂)₂NEt)₃, W(DEEDA)₃) (2). DEEDA (232 mg, 3 mmol) in 10 mL of n-hexane and n-butyl lithium (4.125 mL, 6.6 mmol) were used to generate EtNLi-(CH₂)₂LiNEt *in situ* before the addition of WCl_4(DME) (415 mg, 1 mmol). After filtration, a dark red filtrate was recovered. The filtrate was evaporated under the vacuum to afford a red sticky solid $W(\eta^2$-EtN(CH₂)₂NEt)₃ (272 mg, 52% yield). The complex was further purified by sublimation at 75 °C under 450 mTorr. Data for $W(\eta^2$-EtN(CH₂)₂NEt)₃: ^1H NMR (C_6D_6, 500 MHz): δ 3.99 (m, 12H, CH₃CH_2N−), 3.75 (m, 6H, CH₃CH₂N(CH_2)₂−), 3.42 (m, 6H, CH₃CH₂N-(CH_2)₂−), 1.16 (t, J = 7.02 Hz, 18H, (CH_3)₂N−). ^{13}C NMR (C_6D_6, 125.7 MHz): δ 61.1 (CH₃CH₂N(CH_2)₂−), 55.7 (CH₃CH_2NCH₂−), 16.1 (CH_3CH₂NCH₂−). Anal. calcd for $C_{18}H_{42}N_6W$: C, 41.07; H, 8.04; N, 15.96. Found: C, 40.77; H, 7.89; N, 15.59. Melting point: 153−157 °C.

X-ray Crystallography of 1. Crystals of **1** were grown inside the glovebox from diethyl ether-saturated solution at −20 °C. Paratone oil was coated onto samples of appropriate size and quality before mounting them on capillary glass tubes. Reflection data from the Bruker APEX II-CCD region detector diffractometer were collected using graphite monochromatic Mo Kα radiation (λ = 0.71073 Å). The hemisphere of the reflection data was collected in ω-scan frames with an exposure time of 10 s per frame and a resolution of 0.3° per frame. The SMART program determined and refined cell parameters. SAINT software was used for data reduction. The Lorentz and polarization effects were added to the software data. The SADABS program was used to perform the empirical absorption correction using a direct method. The structure

was solved using a direct approach, and all non-hydrogen atoms underwent anisotropic refinement using the SHELXTL/PC package's full matrix least squares for F^2. Geometrically calculated positions of the hydrogen atoms were used, and isotropic thermal parameters were used for purification. The supplementary crystallographic data for this paper can be found in CCDC 2237298 (**1**). The data can be obtained free of charge from the Cambridge Crystallographic Data Centre (CCDC).

Thermal Analysis of 1 and 2. Thermogravimetric analyses (TGA) of the newly synthesized complexes were conducted using a Thermo Plus EVO II TG8120. TGA was performed in an argon-filled glovebox to avoid air contact; however, the sample might have been exposed to air while connecting the samples for less than 1 min in the TGA apparatus. The TGA data of the complexes were collected and heated at 10 °C/min from room temperature to 550 °C under an Ar atmosphere.

WS$_2$ Thin-Film Deposition. A WS$_2$ thin film on a SiO$_2$/Si substrate was fabricated using chemical vapor deposition (CVD) (Figure S6). The substrate was placed in a crucible with **1** precursor in the center of the CVD furnace. The sulfur powder was placed upstream of the substrate. The substrate was heated to 700 °C, and reactor pressure was maintained at 300 mTorr with a 10 SCCM Ar gas flow. When the substrate temperature reached 700 °C, the sulfur powder was heated to 200 °C using heating tape to introduce the additional sulfur to the WS$_2$ thin film.

ASSOCIATED CONTENT

Supporting Information

The Supporting Information is available free of charge at https://pubs.acs.org/doi/10.1021/acsomega.3c01706.

^{1}H and ^{13}C NMR spectra and DSC plots for all complexes and schematic of CVD growth of the WS$_2$ thin film (PDF)

Accession Codes

CCDC 2237298 contains the supplementary crystallographic data for this study. This data can be obtained free of charge via www.ccdc.cam.ac.uk/data_request/cif, or by emailing data_request@ccdc.cam.ac.uk, or by contacting The Cambridge Crystallographic Data Centre, 12 Union Road, Cambridge CB2 1EZ, UK. Fax: +441223 336408.

AUTHOR INFORMATION

Corresponding Author

   Bo Keun Park − *Thin Film Materials Research Center, Korea Research Institute of Chemical Technology (KRICT), Daejeon 34114, Republic of Korea; Department of Chemical Convergence Materials, University of Science and Technology (UST), Deajeon 34113, Republic of Korea;* orcid.org/0000-0002-4066-0500; Email: parkbk@krict.re.kr

Authors

   Ji Young Son − *Thin Film Materials Research Center, Korea Research Institute of Chemical Technology (KRICT), Daejeon 34114, Republic of Korea; Department of Chemistry, Korea University, Seoul 02841, Republic of Korea*

   Su Han Kim − *Thin Film Materials Research Center, Korea Research Institute of Chemical Technology (KRICT), Daejeon 34114, Republic of Korea*

   Ji Min Seo − *Thin Film Materials Research Center, Korea Research Institute of Chemical Technology (KRICT), Daejeon 34114, Republic of Korea; Department of Chemistry, Sungkyunkwan University, Suwon-si, Gyeonggi-do 16419, Republic of Korea*

   Jongsun Lim − *Thin Film Materials Research Center, Korea Research Institute of Chemical Technology (KRICT), Daejeon 34114, Republic of Korea*

   Taek-Mo Chung − *Thin Film Materials Research Center, Korea Research Institute of Chemical Technology (KRICT), Daejeon 34114, Republic of Korea; Department of Chemical Convergence Materials, University of Science and Technology (UST), Deajeon 34113, Republic of Korea;* orcid.org/0000-0002-5169-2671

Complete contact information is available at:
https://pubs.acs.org/10.1021/acsomega.3c01706

Author Contributions

$^\perp$J.Y.S. and S.H.K. contributed equally to this work.

Notes

The authors declare no competing financial interest.

ACKNOWLEDGMENTS

REFERENCES

(1) Lassner, E.; Schubert, W.-D. The Element Tungsten. In *Tungsten.* Springer, 1999; pp. 1−59.

(2) Kamineni, V.; Raymond, M.; Siddiqui, S.; Mont, F.; Tsai, S.; Niu, C.; Labonte, A.; Labelle, C.; Fan, S.; Peethala, B.; Adusumilli, P.; Patlolla, R.; Priyadarshini, D.; Mignot, Y.; Carr, A.; Pancharatnam, S.; Shearer, J.; Surisetty, C.; Arnold, J.; Canaperi, D.; Haran, B.; Jagannathan, H.; Chafik, F.; L'Herron, B. Tungsten and cobalt metallization: A material study for MOL local interconnects. *IEEE International Interconnect Technology Conference / Advanced Metallization Conference* **2016**, 105−107.

(3) Chen, X.; Zhou, Y.; Liu, Q.; Li, Z.; Liu, J.; Zou, Z. Ultrathin, Single-Crystal WO$_3$ Nanosheets by Two-Dimensional Oriented Attachment toward Enhanced Photocatalystic Reduction of CO$_2$ into Hydrocarbon Fuels under Visible Light. *ACS Appl. Mater. Interfaces* **2012**, 4, 3372−3377.

(4) Drynan, J.; Fukui, K.; Hamada, M.; Inoue, K.; Ishigami, T.; Kamiyama, S.; Matsumoto, A.; Nobusawa, H.; Sugai, K.; Takenaka, M.; Yamaguchi, H.; Tanigawa, T. Shared tungsten structures for FEOL/BEOL compatibility in logic-friendly merged DRAM. *International Electron Devices Meeting* **1998**, 849−852.

(5) Alam, S.; Iqbal, M. Z.; Amjad, N.; Ali, R.; Alzaid, M. Magnetron sputtered tungsten di-sulfide: An efficient battery grade electrode for supercapattery devices. *J. Energy Storage* **2022**, 46, No. 103861.

(6) Yoo, S. J.; Yun, S. U.; Sung, Y.-E.; Ahn, K.-S. Tungsten oxide bilayer electrodes for photoelectrochemical cells. *J. Power Sources* **2010**, 195, 5422−5425.

(7) Choi, W.; Choundhary, N.; Han, G. H.; Park, J.; Akinwande, D.; Lee, Y. H. Recent development of two-dimensional transition metal dichalcogenides and their applications. *Mater. Today* **2017**, 20, 116−130.

(8) Manzeli, S.; Ovchinnikov, D.; Pasquier, D.; Yazyev, O. V.; Kis, A. 2D transition metal dichalcogenides. *Nat. Rev. Mater.* **2017**, 2, 17033.

(9) Dong, R.; Kuljanishvili, I. Review Article: Progress in fabrication of transition metal dichalcogenides heterostructure systems. *J. Vac. Sci. Technol., B* **2017**, *35*, No. 030803.

(10) Han, Z. J.; Murdock, A. T.; Seo, D. H.; Bendavid, A. Recent progress in plasma-assisted synthesis and modification of 2D materials. *2D Mater* **2018**, *5*, No. 032002.

(11) Wu, Y.; Raza, M. H.; Chen, Y.-C.; Amsalem, P.; Wahl, S.; Skrodczky, K.; Xu, X.; Lokare, K. S.; Zhukush, M.; Gaval, P.; Koch, N.; Quadrelli, E. A.; Pinna, N. A Self-Limited Atomic Layer Deposition of WS$_2$ Based on the Chemisorption and Reduction of Bis(*t*-butylimino)bis(dimethylamino) Complexes. *Chem. Mater.* **2019**, *31*, 1881−1890.

(12) Kim, D.-H.; Ramesh, R.; Nandi, D. K.; Bae, J.-S.; Kim, S.-H. Atomic layer deposition tungsten sulfide using a new metal-organic precursor and H$_2$S: thin film catalyst for water splitting. *Nanotechnology* **2021**, *32*, No. 075405.

(13) Campbell, W. R.; Reale, F.; Sundaram, R.; Bending, S. J. Optimisation of processing conditions during CVD growth of 2D WS$_2$ films from a chloride precursor. *J. Mater. Sci.* **2022**, *57*, 1215−1229.

(14) Balasubramanyam, S.; Shirazi, M.; Bloodgood, M. A.; Wu, L.; Verheijen, M. A.; Vandalon, V.; Kessels, W. M. M.; Hofmann, J. P.; Bol, A. A. Edge-Site Nanoengineering of WS$_2$ by Low-Temperature Plasma-Enhanced Atomic Layer Deposition for Electrocatalytic Hydrogen Evolution. *Chem. Mater.* **2019**, *31*, 5104−5115.

(15) Richey, N. E.; Haines, C.; Tami, J. L.; McElwee-White, L. Aerosol-assisted chemical vapor deposition of WS$_2$ from the single source precursor WS(S$_2$)(S$_2$CNEt$_2$)$_2$. *Chem. Commun.* **2017**, *53*, 7728−7731.

(16) Brune, V.; Hegemann, C.; Mathur, S. Molecular Routes to Two-Dimensional Metal Dichalcogenides MX$_2$ (M = Mo, W; X = S, Se). *Inorg. Chem.* **2019**, *58*, 9922−9934.

(17) Smith, D. E.; Greenacre, V. K.; Hector, A. L.; Huang, R.; Levason, W.; Reid, G.; Robinson, F.; Thomas, S. Thioether complexes of WSCl$_4$, WOCl$_4$ and WSCl$_3$ and evaluation of thiochloride complexes as CVD precursors for WS$_2$ thin films. *Dalton Trans.* **2020**, *49*, 2496−2504.

(18) Brune, V.; Grosch, M.; Weißing, R.; Hartl, F.; Frank, M.; Mishra, S.; Mathur, S. Influence of the choice of precursors on the synthesis of two-dimensional transition metal dichalcogenides. *Dalton Trans.* **2021**, *50*, 12365−12385.

(19) Gwildies, V.; Thiede, T. B.; Amirjalayer, S.; Alsamman, L.; Devi, A.; Fischer, R. A. All-Nitrogen Coordinated Amidinato/Imido Complexes of Molybdenum and Tungsten: Syntheses and Characterization. *Inorg. Chem.* **2010**, *49*, 8487−8494.

(20) Rische, D.; Parala, H.; Gemel, E.; Winter, M.; Fischer, R. A. New Tungsten(VI) Guanidinato Complexes: Synthesis, Characterization, and Application in Metal−Organic Chemical Vapor Deposition of Tungsten Nitride Thin Films. *Chem. Mater.* **2006**, *18*, 6075−6082.

(21) Nolan, M. M.; Touchton, A. J.; Richey, N. E.; Ghiviriga, I.; Rocca, J. R.; Abboud, K. A.; McElwee-White, L. Synthesis and Characterization of Tungsten Nitrido Amido Guanidinato Complexes as Precursors for Chemical Vapor Deposition of WN$_x$C$_y$ Thin Films. *Eur. J. Inorg. Chem.* **2018**, *2018*, 46−53.

(22) Chisholm, M. H.; Cotton, F. A.; Extine, M.; Stults, B. R. The Tungsten-Tungsten Triple Bond. 1. Preparation, Properties, and Structural Characterization of Hexakis(dimethylamido)ditungsten-(III) and Some Homologues. *J. Am. Chem. Soc.* **1976**, *98*, 4477−4485.

(23) Blatchford, T. P.; Chisholm, M. H.; Huffman, J. C. Tris(*N,N'*-dimethylethylenediaminato)dimolybdenum and tris(*N,N'*-dimethylethylenediaminato)ditungsten. A Comparison of Eclipsed and Staggered Triple Bonds, $\sigma^2\pi^4$, between Molybdenum and Tungsten Atoms in X$_3$M≡MX$_3$ Compounds. *Inorg. Chem.* **1987**, *26*, 1920−1925.

(24) McClain, K. R.; O'Donohue, C.; Shi, Z.; Walker, A. V.; Abboud, K. A.; Anderson, T.; McElwee-White, L. Synthesis of WN(NMe$_2$)$_3$ as a Precursor for the Deposition of WN$_x$ Nanospheres. *Eur. J. Inorg. Chem.* **2012**, *2012*, 4579−4584.

(25) Yeo, S. J.; Park, B. K.; Kim, C. G.; Chung, T.-M. Synthesis and characterization of tungsten Imido/Aminoalkoxide complexes to deposit tungsten oxide thin films. *Inorg. Chim. Acta* **2020**, *502*, No. 119307.

(26) Persson, C.; Andersson, C. Reduction of tungsten (VI) and molybdenum (V) by allyltrimethylsilane and cyclopentene. Simple high yield syntheses of MoCl$_4$ (OEt$_2$)$_2$, MoCl$_4$(dme), WCl$_4$(thf)$_2$, WCl$_4$(dme) and WOCl$_3$(thf)$_2$. *Inorg. Chim. Acta* **1993**, *203*, 235−238.